EARTH SURFACE PROCESSES AND LANDFORMS, VOL. 21, 641–659 (1996)

CAUSES OF THE FETCH EFFECT IN WIND EROSION

DALE A. GILLETTE

Atmospheric Science Modeling Division, Air Resources Laboratory, NOAA, MD-81, Research Triangle Park, NC 27711, U.S.A.

GARY HERBERT

Climate Monitoring and Diagnostics Laboratory, NOAA, 325 Broadway, Boulder, CO 80303, U.S.A.

PAUL H. STOCKTON

Sensit Labs Incorporated, 879 W. Midway, Mayville, ND 58257, U.S.A.

AND

P. R. OWEN (deceased)

Formerly Zaharoff Professor of Aviation, Imperial College, London, U.K.

Received 22 April 1994
Revised 5 December 1994

ABSTRACT

The increase of soil mass flux with distance downwind, the fetch effect for wind erosion, has been observed and reported on since 1939. This model incorporates the following three mechanisms. (1) The 'avalanching' mechanism in which one particle moving downwind would dislodge one or more particles upon impact with the surface. The result of a chain of such events is an increase of mass flux with distance. (2) The 'aerodynamic feedback' effect, suggested by P. R. Owen, in which the aerodynamic roughness height is increased by saltation of particles; the resulting increased momentum flux increases saltation. These increases define a positive feedback loop with respect to distance downwind. (3) The 'soil resistance' mechanism, which is largely an expression of the change with distance of threshold velocity. Change of threshold velocities may be caused by inhomogeneities of the soil or progressive destruction of aggregates and crust in the direction of saltation fetch.

An experiment was run in March 1993 at Owens Lake to test this model. Detailed measurements of wind profiles and mass fluxes were taken on a line parallel to the wind direction. These data support the proposed three-mechanism model.

KEY WORDS wind erosion; threshold velocity; fetch effect; mass transport

INTRODUCTION

The wind erosion fetch effect, the increase of soil movement with distance downwind from the leading edge of erodible material after the threshold for wind erosion is exceeded, was observed by Chepil and Milne (1939). Soil flux, q, is measured as mass of soil particles passing through an area perpendicular to the ground, normal to the wind, and of unit width extending to the top of the atmosphere. Chepil (1957) explained the effect as 'avalanching' in which the saltation (hopping) motion of a sand particle sets more than one sand particle into motion after travelling a hop distance. A chain of such events was visualized by Chepil to resemble the avalanching of snow. For constant wind stress and a constant number of particles dislodged by one impact, such an explanation leads to the prediction of an exponential growth in sand movement measured downwind. That is, the horizontal flux, q, of soil increases exponentially until it comes to a 'saturation' where sand movement near the ground carries all the vertical momentum flux from the wind. With regard to snow, the fetch effect has been observed as an increase in the quantity of snow transported with distance (fetch) from stable snow up to fetches of 300 m for low wind speeds and 1000 m for high wind speeds, after which the effect of

CCC 0197–9337/96/070641–19

sublimation of snow particles decreases the transported snow (Pomeroy *et al.*, 1993). Gregory and Borrelli (1986) expressed the increase of flux as an exponential increase using dimensional analysis to predict soil mass detached by airflow. Stout (1990) derived a similar semi-empirical expression for exponential increase of soil flux,

$$f(x,z) = f_{\max}[1 - \exp\{-x/b(z)\}]$$

where f is mass flux of soil particles at a given height z and downward distance x, $f_{\max}$ is the maximum of that flux, and b is a function only of z.

The relationship between $f(x,z)$ and $q(x)$ is

$$q(x) = \int_0^H f(x,z)\mathrm{d}z$$

where H is the top of the particle-containing layer. Stout derived an expression for b by rewriting the equation of mass conservation for sand by assuming that the first derivative divided by the second derivative of horizontal sand flux with respect to fetch distance is a function only of height. The variable $b(z)$ was interpreted by Stout (1990) as an entrainment coefficient for loose saltation-size material. Since b has the units of length, it is also interpretable as the distance at which the flux reaches 63 per cent ($1 - e^{-1}$) of its maximum. The exponential form fitted rather well extensive data for the increase of sand flux with fetch for a circular sandy farm field in Big Spring, Texas; however, the values of b changed with height and with individual storms. The value of b was typically tens of metres to 100 m for homogeneous sand at Big Spring (J. E. Stout, U.S. Dept. of Agriculture, Agricultural Research Service, pers. comm., 1993). Shao and Raupach (1992) also found variation of q with downwind distance in a wind tunnel and successfully modelled it using the model of Anderson and Haff (1991). This model showed that a fetch of several metres was required for q to come to an equilibrium value. The scale of this effect for the wind tunnel work of Shao and Raupach was of the order of metres for homogeneous sand deposits. The above observations suggest that the avalanching effect may explain the wind erosion effect for distances of a few tens of metres from the edge of the erodible material but that other mechanisms may be required for a larger-scale fetch effect.

Bradley's (1968) experimental data on adjustment of shear stress to an abrupt change of roughness for the transition from a rough surface to a smooth surface showed that the friction velocity adjusted rapidly so that an equilibrium value was reached within 2 to 4 m after the change. The very small adjustment distance precludes this mechanism as a cause of the large-scale fetch effects described above.

Two mechanisms possibly causing a larger-scale fetch effect were proposed by two of the co-authors of the present paper. One of the co-authors (P. R. Owen) suggested that the cause of the fetch effect was an aerodynamic feedback effect with respect to distance downwind. (See Acknowledgements.) That is, he suggested that saltating sand grains could increase the apparent aerodynamic roughness height. This increase of roughness height leads to an internal boundary layer in which more momentum is transferred to the surface. In Owen's theory, the increased momentum flux to the soil leads to an increased particle flux that further increases the aerodynamic roughness height. These interactions constitute a positive feedback of increasing momentum flux with distance downwind. Since the square of friction velocity, $u*$, times air density is equal to momentum flux, this results in an increase of $u*$, with fetch distance.

Another of the co-authors of the present paper (D. A. Gillette) suggested that a mechanism for the fetch effect is change of the soil's resistance to erosion with distance. This effect followed from observations of Gillette and Stockton (1989), which showed that as the fraction of the frontal area of non-erodible particles decreased, more of the wind momentum flux went to transporting soil through the air. Because soil aggregates (including soil crusts) would be expected to be increasingly destroyed by sandblasting, which itself grows as a function of distance from the leading edge, the same wind stress could transport more airborne soil mass as distance increased from the leading edge. The change of soil resistance to wind erosion with distance is observable as a change of the percentage of the surface as crust. Because Gillette and Stockton (1989) showed that threshold friction velocity also decreased with destruction of surface crusting, this effect could be detected as a decrease of threshold friction velocities with distance downwind.

The purpose of this paper is to determine the relative importance of the three mechanisms described

above. The mechanisms must explain both small-scale and large-scale (greater than tens of metres) fetch effects and the increase or decrease of q with downward distance. We propose that three mechanisms work together to bring about the wind erosion effect: avalanching, aerodynamic feedback, and soil resistance.

We test a (conceptual) model incorporating the three mechanisms versus a model that invokes only the avalanching mechanism. This comparison is undertaken because the avalanching mechanism is widely accepted to be the sole cause of the wind erosion fetch effect, and we would like to point out the importance of the aerodynamic feedback and soil resistance mechanisms. The two models are tested for scales of hundreds of meters in a natural outdoor setting.

MODELS FOR WIND-EROSION FETCH EFFECT AND TESTS OF THE MODELS

Equations of the avalanching model and the avalanching aerodynamic feedback/soil resistance model

The pure avalanching model (model 1) may be written as

$$q(x) = F(x)q_{\max} \tag{1}$$

where $q_{\max}$ is not a function of x. $F(x)$ is a positive number, and is similar to Stout's $f(x)$ term in the Introduction. The quantity $q_{\max}$ may be written as Owen's (1964) solution of the equations of mass and momentum conservation for an air/particle system:

$$q_{\max} = A\frac{\rho}{g}u_*(u_*^2 - u_{*t}^2)$$

where ρ and g are density of the air and gravitational acceleration, respectively, A is a constant, and u_{*t} is threshold friction velocity. Using this equation, Equation 1 becomes

$$q(x) = F(x)A\frac{\rho}{g}u_*(u_*^2 = u_{*t}^2) \tag{2}$$

Model 1 (pure avalanching) requires u_{*t} and u_* to be constant with x. Model 2, the avalanching/aerodynamic feedback/soil resistance model allows change of u_{*t} with x and change of u_* and z_0 with x as effected by airborne sand grains.

Tests of the models

The following tests were made for the two models for conditions when the erosion threshold was exceeded for all locations and where there was a measurable change of soil flux q with distance downwind.

The avalanching model (model 1). (1) The direction of q increase is always downwind. That is, $F(x)$ must be greater than 0 and must increase with distance downwind. (2) Friction velocity and threshold friction velocities are constant,

Avalanching/aerodynamic feedback/soil resistance model (model 2). (1) For some range of u_*, aerodynamic roughness height increases with friction velocity (and saltation flux). For this range of u_*, u_* should increase downwind. (2) Disaggregation of the soil (alternately u_{*t}) decreases in the direction that q increases. (3) An avalanching effect is identified from the data by $q/[u_*(u_*^2 - u_{*t}^2)] = A'F(x)$, where A' is a constant (equal to $A\rho/g$). $F(x)$ must be non-random and increase with x. In a case where u_{*t} increases with fetch, transport of sand will modify the decrease of q such that q decreases less rapidly with distance (overshoot of q.)

EXPERIMENTAL DETAILS

The tests in the previous section require measurement of soil flux, wind friction velocity and aerodynamic roughness height, and threshold friction velocity. Because the severely abrasive atmosphere is extremely damaging to sensitive instrumentation, instruments were chosen for ruggedness as well as precision. On the basis of many years of experience in outdoor wind erosion measurements, it was decided to measure friction velocity and aerodynamic roughness height by the wind profile method using the most sensitive anemometers that we thought would withstand the sandblasting of the wind erosion episodes. Soil flux was

measured with instrumentation developed for agricultural wind erosion measurements. The experiment was at a site having frequent high winds and erodible soils.

Owens Lake setting

The primary site of the experiment conducted in March 1993 was on an erodible part of the Owens (dry) Lake floor near the town of Olancha, California. A map showing the location of Owens Lake is given by Cahill *et al.* (1996). A secondary site on another part of the erodible lake floor near the town of Keeler, California, was used for feasibility tests in May 1991. Owens Lake had an area of 300 km^2 and was fed by the Owens River. However, in 1913, the newly completed Los Angeles Aqueduct diverted by the entire flow of the Owens River to Los Angeles. At the present time, only small areas of the lake are fed by seeps and ephemeral drainages, with the result that the entire lake bed is virtually dry. The lake bed is composed of large areas of sandy flat areas, crusts, dunes, and clay-rich flats. The area chosen for the experiment was a loose, sandy, flat area immediately downwind of a crusted flat area. Both the upwind and sandy flat areas were totally unvegetated and devoid of topography. Visually, the upwind crusted area was of about the same flatness as the loose area. An analysis of the surface material at the primary site is shown in Figure 1, which shows a gradient for sand content from north to south. Such a gradient in composition can give rise to a gradient in crust strength (Gillette *et al.*, 1981), with crust strength increasing to the north. The soil at the secondary site consisted of (by mass) 0·54 per cent organic material, 10 per cent carbonate, and 9·13 per cent soluble salts. A size analysis of the surface material for 11 sites of the north–south line of the primary site and the secondary site of the feasibility study is given in Table I. Soil pH values were 9·6 at the secondary site and 10·0 ± 0·1 at the 11 points of the primary site.

Meteorological profile measurements

Instrumented towers were on a north–south line along the dominant wind direction. Predictions of the location of the strongest fetch effect were based on the 1991 preliminary experiment and repeated examination of the surface from May 1991 until 1993. Four instrumented towers of a design of one of the authors (G.H.) were set at the points 0, 50, 100 and 150 m on the line. Two instrumented towers of a design of another of the authors (P.S.) were set at measured distances of 520 and 1057 m. For the 1991 feasibility test, the same two towers were set at distances of 77 and 442 m downwind of the leading edge of the erodible sandy material from the edge of the non-erodible crusted material.

On the first four towers, wind measurement were taken by using Climet light chopping cup anemometers

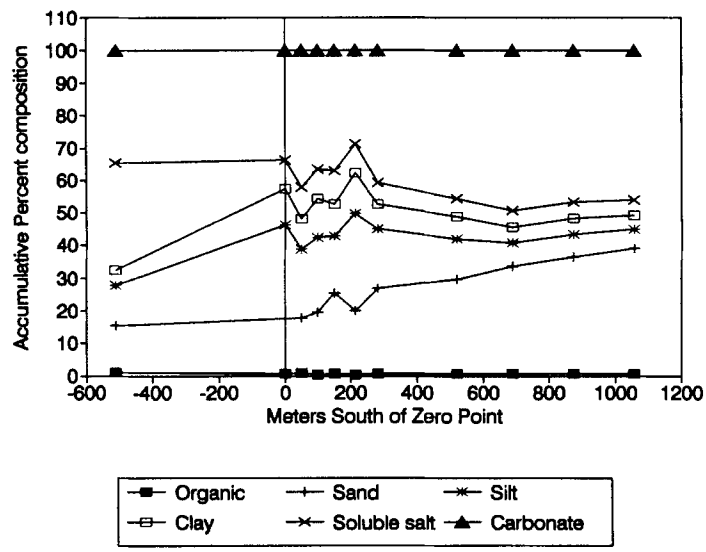

Figure 1. Soil properties as a function of distance south of the zero point. The six components add to 100 per cent by mass

Table I. Percentage of mass in size intervals (upper and lower in micrometres) for the May 1991 test and March 1993 tests by distance south (in metres from the zero point)

To	2000	1000	500	250	100	50	20	10	5	2	<1
From	1000	500	250	100	50	20	10	5	2	1	
May 1991 data											
	23·3	11·9	16	30·3	14·4	1·8	0·4	0·4	0·5	0·3	0·8
March 1993 data											
−510	0·6	0·5	8·3	25	11	7·2	7·1	11	15	6	8·8
0	1·5	0·7	5·1	15	7·8	8	9·5	16	17	7·9	12
50	2·3	2·3	6·7	16	8·3	6·6	8·2	14	16	7·4	12
100	0·2	3·3	12	14	5·9	6·9	7·1	13	16	8·6	13
150	1·2	11	20	10	5·3	5·6	5·6	8·8	14	7·2	11
213	1·3	1·9	7·2	14	7·2	8·3	7·4	14	19	9·1	11
282	0·9	2·4	15	23	9	4·7	7·8	10	12	5·7	8·9
520	0·3	6·1	23	24	7·4	4·1	4·2	7	10	5·2	8·9
691	0·4	15	31	20	6·8	2·8	2·8	4·4	5·7	3·6	7
874	0·2	8·1	30	30	7·3	2·2	3	3·9	5·3	3·6	6·8
1056	0·5	8·1	40	25	6·1	2·3	2·5	3·2	4·3	2·7	5·9

(model 011-4). The threshold was 0·33 m s^{-1} and accuracy was ± 1 per cent for the range 0–40 m s^{-1}. The distance constant of the anemometers was 1·5 m. The heights of measurements were 20, 50, 100 and 300 cm. The instruments were carefully chosen from a pool of 67 units to have matched response to the wind. This testing allowed anemometers to be matched to within ± 3 per cent. Testing of the anemometers at uniform height took place at a uniform height on Table Mountain, Colorado (a flat, elevated mesa), north of Boulder, Colorado, in October and November 1992. Calibration of selected anemometers was done in the National Center for Atmospheric Research calibration wind tunnel in Boulder. One-minute-average speeds were recorded for all four instrumented towers using a laptop computer-based data-logging system. The system was contained in a dust-proof case and was powered by sealed batteries.

The towers located at 520 and 1057 m south of the zero point had the following instruments: four anemometers at 20, 50, 100 and 200 cm height, an external system thermometer, and a wind direction sensor. The anemometers were calibrated as above. The instruments were controlled and data was stored using a computer-controlled data system capable of storing 1 M of digital data. Each tower was powered by a 45 W solar panel that used a 36 ampere-hour sealed storage battery.

Soil flux measurements

Soil flux measurements were taken using six BSNE collectors at each instrumented tower location. In between the 520 and 1057 m instrumented towers, we placed a six-BSNE collection station at 874 m. The collectors and their calibration were described by Fryrear (1986). These collectors were passive collectors that maintained 90 per cent efficiency for all winds (Shao *et al.*, 1993) because of top-venting and the large Stokes numbers of the soil particles being collected. Soil flux was collected at six individual heights, 10, 20, 30, 50, 60 and 100 cm above the surface, for sampling times of from 1 to 5 h. A simple model of sampler efficiency (Stokes number greater or equal to 1) yielded 100 per cent efficiency for the BSNE sampler for unit density particles larger than 20 μm and radius of curvature of 0·5 cm to escape the BSNE intake at a wind speed of 5 m s^{-1}.

In addition, at the 520 and 1057 m locations, erosion kinetic energy sensors (Sensits) were placed at heights of 5, 10, 30 and 50 cm from the ground surface. These sensors were previously used by Stockton and Gillette (1990) to sense airborne sand movement.

Data processing estimation of errors

Data sets obtained for the verification of the models were friction velocity, aerodynamic roughness height, and integrated mass flux Q (defined below in Equation 6).

Friction velocity and aerodynamic roughness height. Friction velocity was calculated for each 20 min period by finding the 20-min average wind speed at the four heights, $z = 20$, 50, 100 and 300 cm for the first four

towers and $z = 20$, 50, 100 and 200 cm for the towers located at 520 m and 1057 m. The least-squares fit of mean wind speed to the natural logarithm of height z was used with

$$U(z) = 2{\cdot}5u_* \ln(z/z_0) \tag{3}$$

to compute friction velocity, where z_0 is aerodynamic roughness height (Panofsky and Dutton, 1984). The 90 per cent confidence interval (*CI*) for the estimate of friction velocity was related to the standard error of the regression s_{err} (Miller and Freund, 1977) as

$$CI = \pm t_{\alpha/2} S_{\text{err}} \sqrt{(n/s_{\text{xx}})}$$

where

$$s_{\text{xx}} = n \sum_1^n x_i^2 - \left(\sum_1^n x_i\right)^2 \tag{4}$$

where x_i is the independent value of the regression (in our case the natural logarithm of height), n is the number of observations and $t_{\alpha/2}$ is the t statistic for the $\alpha/2$ level, where $\alpha/2$ is half the level of significance. The 90 per cent confidence interval (*CI*) for aerodynamic roughness height (the height at which the extrapolated value of mean wind speed goes to zero) was calculated as

$$CI = \pm \exp\left(t_{\alpha/2} S_{\text{err}} \left[\left[1 + \frac{1}{n} + \frac{n[-(a/b) - \bar{x}]^2}{S_{\text{xx}}} \right]^{1/2} - a \right] / b \right) \tag{5}$$

where a and b are the constant and coefficients, respectively, of the linear regression, $\bar{x}$ is the mean of the x_i and n is as above.

Threshold friction velocity. Threshold friction velocities were the friction velocities above which soil eroded *steadily* (not intermittently) during the sampling period. Threshold friction velocities were estimated by carefully noting when the threshold for erosion was reached or when it stopped. Because the surface was disaggregated by the several wind erosion episodes between 11 and 25 March, threshold velocity decreased during that time. From 12 to 15 March several small episodes slightly above or slightly below threshold, which were too short in duration and too weak to break down the surface aggregation, allowed us to make more than one estimation when threshold was reached. The estimates of error for threshold friction velocity follow the estimates of error for friction velocity.

Soil mass flux. The fluxes collected at six individual heights (10, 20, 30, 50, 60 and 100 cm above the surface) were interpolated using the formula used by Shao and Raupach (1992), $c\exp(az + bz^2)$, where a, b and c are constants. The fits of the data to the formula gave an average value of r^2 of 0·96 with standard deviation 0·027. There were no apparent differences of r^2 with location or sampling time. because fluxes were obtained over a finite time interval, the measurements were represented by

$$Q = \int_0^t q\mathrm{d}t \tag{6}$$

The estimate of the 90 per cent confidence interval for the Q was $t = 0{\cdot}05$ (three degrees of freedom) times the standard error of the least-squares fit evaluated at the height of the maximum flux. Because the standard error did not vary with time or location, we estimated the 90 per cent confidence interval for Q to be 9 per cent of the Q value.

The quantity G. Because the soil mass fluxes were measured over finite periods, to make the wind data consistent for comparison with the soil flux data, we defined G as follows:

$$G = \int_0^t u_*(u_*^2 - u_{*\text{t}}^2)\mathrm{d}t \tag{7}$$

The error assigned to each G estimate was related to the errors of both the friction velocity estimate and the threshold friction velocity by examination of Equation 2. For no error in $F(x)$, small fractional errors in

threshold friction velocity and friction velocity result in the fractional error of G as

$$\Delta G/G = [(3 - B^2)y + 2Bs]/(1 - B^2) \tag{8}$$

where $B = u_{*t}/u_*$, $y = \Delta u_*/u_*$, and $s = \Delta u_*/u_*$. For u_* greater than u_{*t}, the error is approximately three times the error of the friction velocity. For friction velocity near the threshold, small errors in both threshold friction velocity and friction velocity are magnified by $1/(1 - B^2)$.

RESULTS

Soil mass flux

Integrated soil mass fluxes Q were obtained for 12 wind erosion time periods during the March 1993 testing period and one 5 h long erosion episode during the preliminary testing period of 17–18 May 1991. Data from all these cases showed an increase of Q from north to south. Selection of the data sets from among the 13 possible cases was based on the following three criteria:

(1) wind direction was within 10° of the line of the sampling towers;
(2) wind erosion was fully developed at all sampling towers, and wind friction velocities were at or above threshold for wind erosion;
(3) more than two points of data were required for an erosion episode.

Prior to 11 March 1993, the boundary between the fully crusted material and the partially crusted soil was at 75 m. On 11 March, high winds broke the crust back to a distance 503 m north of the zero tower at 10:00 local standard time (LST). That boundary was stable until 25 March when the experiment was terminated by heavy rain. Therefore, 503 m should be added to the distances from the northernmost tower after 11 March to give the distance to the south of each tower from the crust/broken crust and loose material boundary. From the crust/broken crust boundary to the south, there was a continuous gradation of crustal destruction to the point of no visible crust. The point of no visible crust moved from 11 March until 25 March as the destruction of the partially disaggregated crust steadily proceeded during dust storms.

Seven wind erosion episodes were eliminated using the above three selection criteria including one when wind was from the northwest (17 March 1993), five when two or more of the locations were below threshold, and the set in 1991 which had only two sampling points. The selected six data sets of Q versus distance south from the farthest north tower are shown in Figure 2.

These data represent north winds (denoted by N in Figure 2) that were experienced on 11 March, before and after 1200 LST (denoted AM and PM in Figure 2), and on 18 March. South winds were experienced on 16 March, 23 March AM and 23–25 March. Q increases from north to south, regardless of the wind direction. The episodes with southerly winds clearly refute model 1. The steepest gradients of Q versus x occurred on 11 March, immediately following the break-up of the crust when the surface was in its most aggregated condition. For north winds on 18 March, the gradient is smaller and the surface was more homogeneous with respect to pulverization. The smallest gradients of Q versus x occurred for south winds on 16, 23 and 23–25 March when the surface aggregates had been pulverized by several wind erosion episodes and the direction of sand transfer was parallel to the gradient of more-pulverised to less-pulverized. For x greater than 150 m, very little gradient of Q with x is seen. Therefore, the data for $0\text{ m} < x < 150\text{ m}$ were of primary interest for this analysis.

Aerodynamic roughness heights

Detailed measurements of wind profiles for $0\text{ m} < x < 150\text{ m}$ for sets satisfying the above selection criteria were examined for quality of the wind profile data. The ratio of standard error of the friction velocity estimate divided by the friction velocity estimate was used to judge profile quality. An example of a wind profile meeting the selection criteria during an erosion episode (09:49 on 11 March 1993) is given in Figure 3. Mean values of these ratios for the first four towers (0, 50, 100 and 150 m locations) for 11 March were 3, 3, 1 and

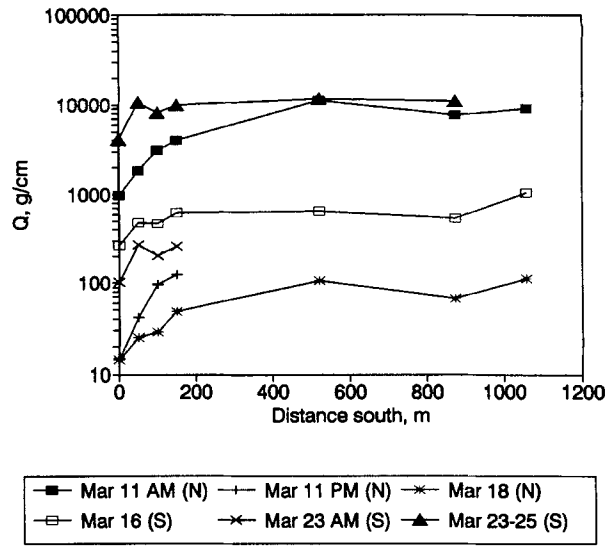

Figure 2. Integrated soil mass fluxes versus distance south of the zero point for selected data sets. N and S denote north and south winds, respectively; AM and PM denote before and after 12:00 LST. respectively

1 per cent, respectively. On 18 March the ratios increased to 36, 14, 8 and 4·6 per cent, respectively. On 23 March, the mean ratios were 20, 13, 33 and 27 per cent, respectively. The data clearly show a degradation of quality with time, probably caused by accumulating bearing friction in the extremely abrasive atmosphere. To use our best data, we emphasized the 11 March observations for all four locations and the 18 March data for the 50, 100 and 150 m locations. The poorer quality data from 23 March AM were also used because they were our best representative data for south winds.

Figure 4 shows the estimated aerodynamic roughness heights for $x < 520$ m along with the 90th percentile confidence interval for the 150 m downwind location. Only the upper limit of the confidence interval is shown, the lower limit being zero. During a time interval from about 09:30 to 11:00 LST, z_0 is higher at every measurement location than z_0 at 08:00 or 12:00 LST. For all five locations the aerodynamic

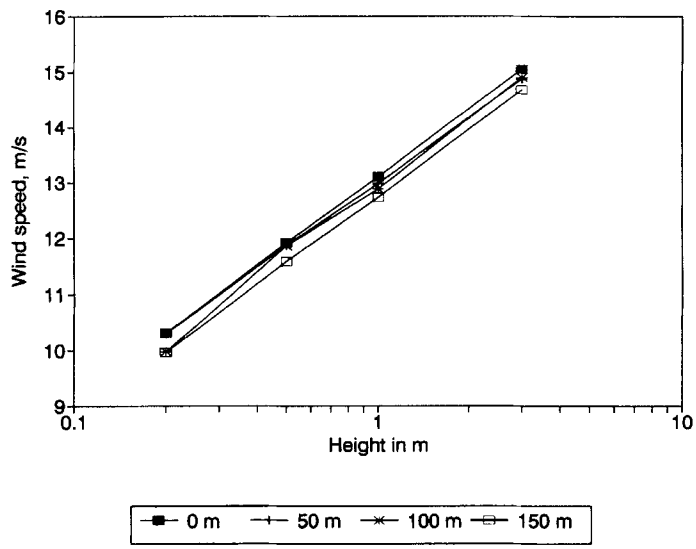

Figure 3. Profiles of wind speed versus height for $x < 200$ m. Data were obtained during a strong wind-erosion episode on 09:48 LST on 11 March 1994

roughness height increased during higher wind friction velocities (see next section) compared with aerodynamic roughness heights for lower wind friction velocities. Furthermore, although not significant, the data suggest larger z_0 for downstream locations compared with upstream locations, in agreement with Owen's theory.

The above suggestion is bolstered by the quantity of data in the plot: although individual point values of z_0 are not significant, a large number of z_0 points show a consistent increase with fetch from 09:30 to 11:00 and this relationship is obliterated after 12:00. Thus an argument that the above pattern was caused by stability-based errors in the slope of the wind profile seems to be improbable because of the correspondence of the pattern only with the most extreme friction velocities of the entire experiment, the fact that meteorological conditions of cloudlessness implied that solar flux increased monotonically during the morning (not just from 09:30 to 11:00), and the fact that the five experimental locations had well-matched instrumentation located within 520 m of each other.

Figure 4 also shows the decrease of z_0 occurring after 05:00 for all five locations, corresponding to the progressive pulverization of the soil crust following the initiation of erosion. Before 06:00 LST, the z_0 values of around 0·1 cm are typical for the crusted surface of sites from zero to 150 m downwind. After 05:30 and before 08:00 LST the z_0 values for locations $x < 200$ m decreased with the destruction of crust by sandblasting. A smoother and thinner crust at 520 m is reflected in the smaller z_0 value (about 0·07 at 04:30) when erosion began. Continuous sand flux data showed that the crust at 520 m broke rather quickly (see Figure 10); the broken crust—now sand mixed with broken crust pieces—is reflected in the reduced z_0 value of about 0·05 cm. Continued sandblasting of the crust during the day reduced the aerodynamic roughness height for all of our sites from about 0·03 to 0·06 cm at 08:00. Following the intense sandblasting of 09:30–11:30 LST, z_0 ranged from about 0·01 to 0·03 cm and there was no significant z_0 difference among the five locations.

Following the 11 March erosion event, erosion events further pulverized the surface soil aggregates, resulting in aerodynamic roughness heights smaller than 0·01 cm at all the measuring locations. The next significant erosion event following 11 March occurred on 18 March with strong winds from the north. Figure 5 shows values of z_0 for the 18 March erosion episode for locations 0 to 150 m downwind and the 90th percentile confidence interval (the lower limit being zero) for 150 m. It will be noted in the next section that friction velocity at any measuring location did not exceed 30 cm s^{-1} during the erosion episode. During the erosion period on 18 March, z_0 values were not greatly different for the four locations and no distinct period of increased aerodynamic roughness height was found.

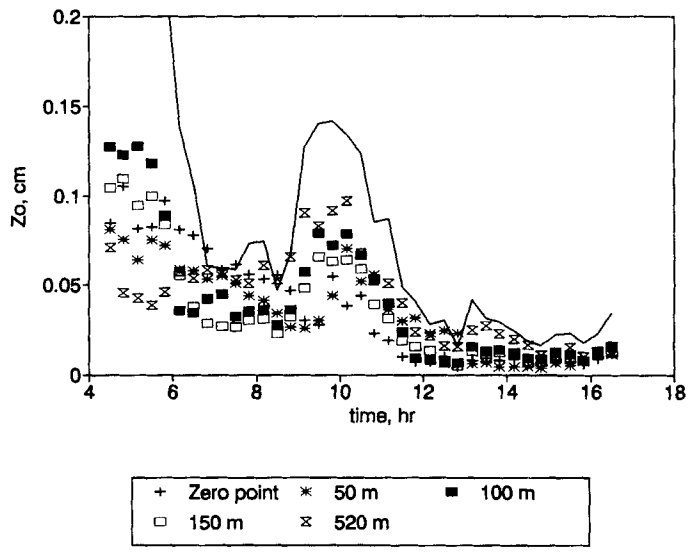

Figure 4. Aerodynamic roughness height for five sampling locations versus time on 11 March 1993. The solid line indicates the 90th percentile confidence interval upper limit for the 150 m location. The lower limit of the 90th percentile confidence interval is zero

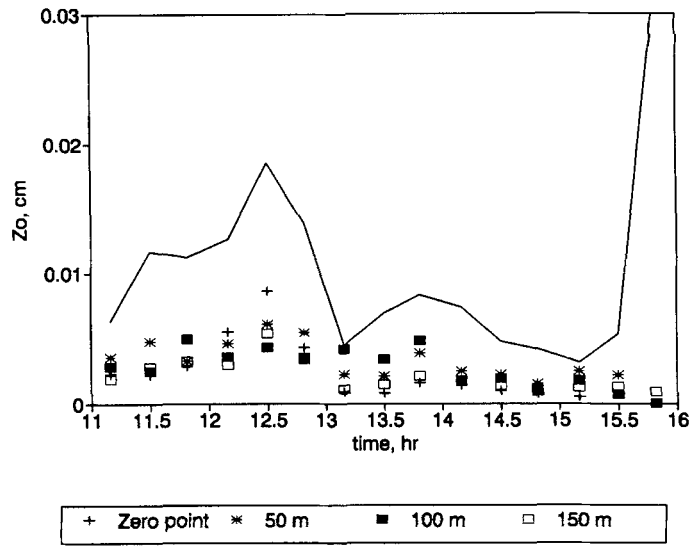

Figure 5. Aerodynamic roughness height for four sampling locations versus time on 18 March 1993. The solid line indicates the 90th percentile confidence interval upper limit for the 150 m location. The lower limit of the 90th percentile confidence interval is zero

Friction velocity

Figure 6 shows the friction velocities for $x < 520$ m during the storm of 11 March 1993 and the 90th percentile confidence intervals for the 150 m value. At the most intense period of the storm (shortly before 10 : 00 LST when all the sampling locations showed an increased aerodynamic roughness height), the friction velocities at 100 and 150 m downwind appear higher than those at the zero point and at 50 m. To distinguish a 90 per cent significant difference between the friction velocities at the zero point and 150 m locations, the difference would need to exceed the sum of 90 per cent confidence intervals for both locations. Indeed, individual pairs of u_* measurements show significant differences for three 20 min intervals during the time interval of maximum wind speeds (09 : 00–11 : 00 LST). One of these three 20 min intervals is shown in Figure 7 as

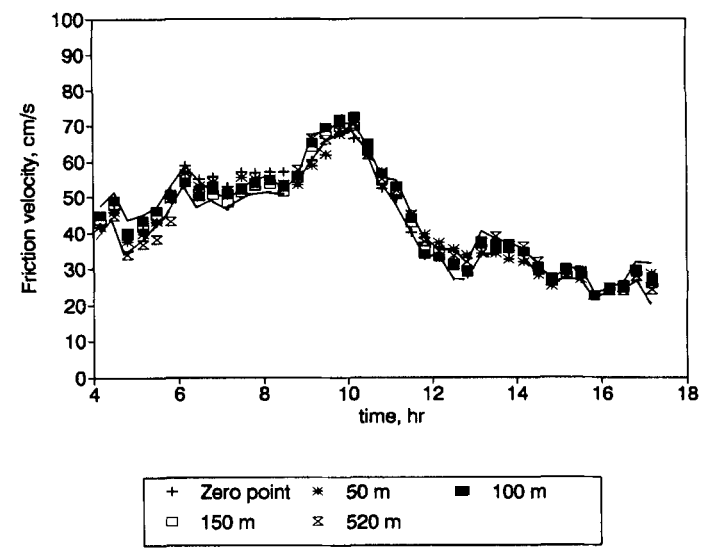

Figure 6. Friction velocities for five sampling locations versus time on 11 March 1993. The solid lines indicate the 90th percentile confidence interval for the 150 m location

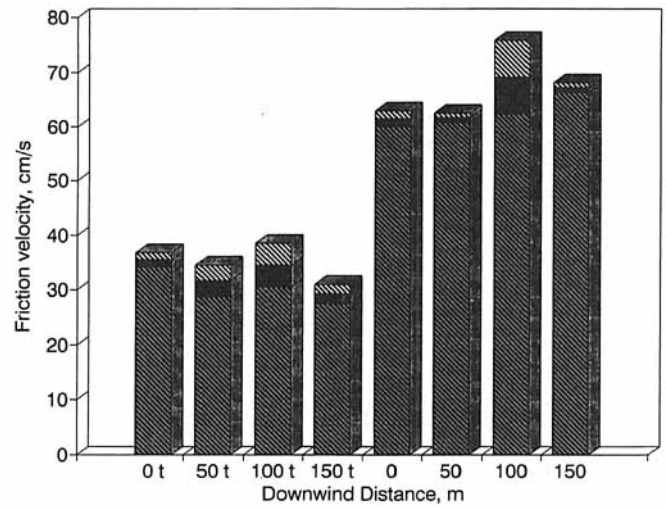

Figure 7. Threshold friction velocities (labelled 't' on x axis) for 11 March 1993 and friction velocities for 09 : 30 LST for the same day. The x axis shows a distance downwind from the first measuring location. The bars indicate the 90th percentile confidence interval for each estimate

stacked bars representing mean and lower and upper 90th percentile confidence intervals for friction velocity during the time interval centred at 09 : 30. The data show that friction velocity is significantly larger at 150 m compared to that at 0 m, and suggest that friction velocity is larger at 100 m compared to that 0 or 50 m (but not significantly). A significant friction velocity increase with downwind distance (fetch) coupled with a significant z_0 increase with friction velocity time (10 : 00 compared to 08 : 00 or 12 : 00 LST) provides support for Owen's theory of the fetch effect. The friction velocity data do not show a significant difference after 12 : 00 LST when wind speeds were lower and aerodynamic roughness heights were approximately uniform for all the measurement locations. Data taken before 08 : 00 show the effect of the rough-crusted surface and its destruction in the first few hours of the storm. The most crusted locations (farthest north) have larger aerodynamic roughness heights and friction velocities than the less crusted 520 m location.

Figure 8 shows the friction velocities for $x < 520$ m during the storm of 18 March 1993 and the 90th percentile confidence intervals for the 150 m value. For the 18 March case, the friction velocity did not significantly differ with downwind fetch, although Q increased with fetch. Another wind erosion episode during the morning of 23 March 1993 showed the same lack of significant difference for friction velocities for $0 < x < 150$ m, when wind of about the same strength as during 18 March came from the south. During the episode of 23 March, Q decreased with distance downwind.

Threshold velocity results

From 11 March after 16 : 00 LST until 15 March 1993, several wind erosion episodes in which the friction velocity was just above threshold for one or more of the locations gave us the opportunity to make several observations of u_{*t} for $0\,\text{m} < x < 150\,\text{m}$. These threshold friction velocities with 90 per cent confidence intervals (shown in Figure 7) were 35·5 (1·3), 31·7 (2·9), 34·6 (4·1) and 29·3 (1·8) cm s^{-1} for the 0, 50, 100 and 150 m locations, respectively. These values allow only the following inequality at the 90 per cent confidence level: $u_{*t}(0\,\text{m}) > u_{*t}(150\,\text{m})$.

The threshold friction velocities for $x \leqslant 520$ m measured from 11 March until 25 March, which were calculated by least-squares fits of four levels of 20-min-averaged wind speeds, are given in Table II along with percentage of the surface as unbroken crust. The state of the crust progressed from being initially homogeneous to fairly thoroughly pulverized soil by 23 March. Table II shows that the north–south gradient of threshold velocity and percentage of surface as crust was steepest on 11 March and smallest at 23 March. Figure 9 shows that the measured percentage of surface area as crust fragments correlates well with u_{*t}, for the

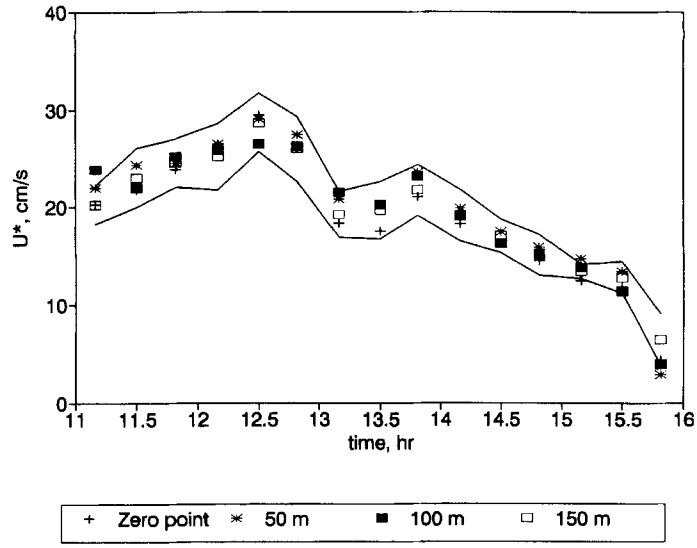

Figure 8. Friction velocities for four sampling locations versus time on 18 March 1993. The solid lines indicate the 90th percentile confidence interval for the 150 m location

March 1993 Owens Lake experiment. Explained variance r^2 was 0·93 for 20 degrees of freedom. The regression equation shown in Figure 9 is

$$u_{*t} = 24{\cdot}0 + 0{\cdot}292 \text{ (\% of surface of crustal fragments) (cm s}^{-1}\text{)}$$

Standard error of the u_{*t} estimate is 3·2 cm s^{-1}. Progressive destruction of the crust with distance suggests a decrease of u_{*t} with fetch distance.

Fast-response instrumentation in place on 11 and 18 March at the 520 m location showed the reduction of u_{*t} discussed above. Figure 10 shows the Sensit response *versus* estimates of u_* for 2-min-average periods. The 2 min u_* values were calculated from 2-min-average wind speeds and using Equation 3. The use of 2-min-averaged estimates of u_*, while insignificant for point-by-point comparison, does suggest, by the consistency of its overall pattern of more than 250 points, that the threshold friction velocity has changed significantly in the course of 11 March 1993. Whereas errors caused by large-scale eddies and thermal effects could affect individual points, the overall pattern of data suggests a significant change of threshold friction velocity. Sensit response was 100 for no particle impacts and above 100 for detectable particle flux. Figure 10

Table II. Percentage of surface as crust and threshold friction velocities, at five locations, March 1993

Date	0 m	50 m	100 m	150 m	520 m
Percentage of surface as crust					
11 March (AM)	100	100	100	100	100
11 March (PM)	33	20	14	3	2
16 March	16	13	10	2	6
17, 18 March	11	7	8	4	6
19–25 March	8	4	4	2	3
Threshold friction velocities in (cm s^{-1})					
11 March (AM)	60	55	50	50	50
11 March (PM)	35·5	31·7	34·6	29·3	18
17 March	29	27		26	
18 March	27	25	25	25	
19–25 March	27	24	24	24	

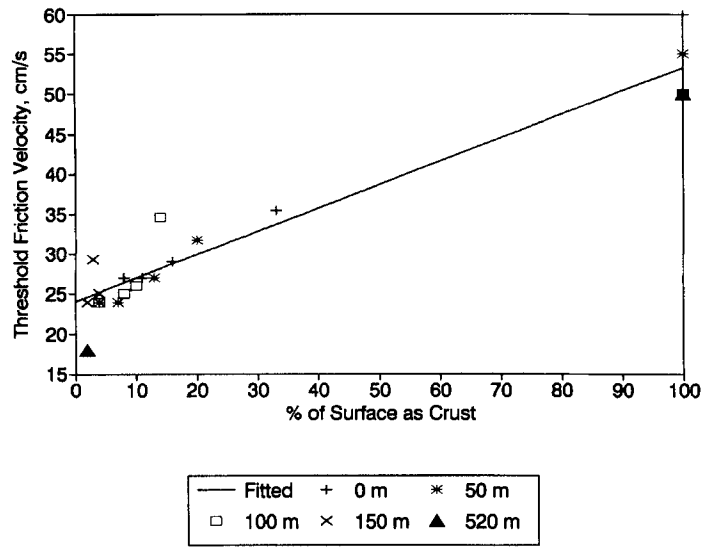

Figure 9. Threshold friction velocity versus percentage of the surface as crust fragments for the March 1993 experiment for locations at 0–520 m

shows that prior to destruction of the crust for the 520 m location, the approximate u_{*t} value was 50 cm s^{-1}. Shortly after the crust was broken, the apparent value of u_{*t} (roughly obtained by following the locus of 'before 12:00' LST data points to Sensit response = 100) dropped to about 23 cm s^{-1}. The reduction of almost 30 cm s^{-1} in threshold friction velocity appears to have taken place in just a few minutes. The approximate value of u_{*t} for the 'after 12:00' LST points was about 18 cm s^{-1}. Another interesting feature of Figure 10 is an apparent flattening of the response for friction velocity greater than 60 cm s^{-1} compared to that for 40–60 cm s^{-1}. This response curve suggests that the mass flux q deviates from q *versus* $u_*(u_*^2 - u_{*t}^2)$ for $u_* > 60$ cm s^{-1}, this measurement is only the flux at 10 cm rather than for the entire saltation height, however. Figure 10 shows Sensit response *versus* 2-min-average estimates of u_* for the 1057 m loca-

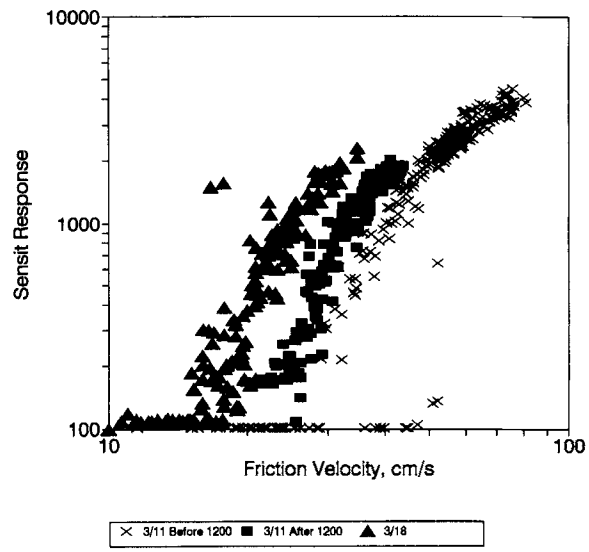

Figure 10. Two-min Sensit response versus two-point friction velocity for 11 March 1993 (location 520 m south of the zero point), and for 18 March 1993 (location 1056 m south of the zero point)

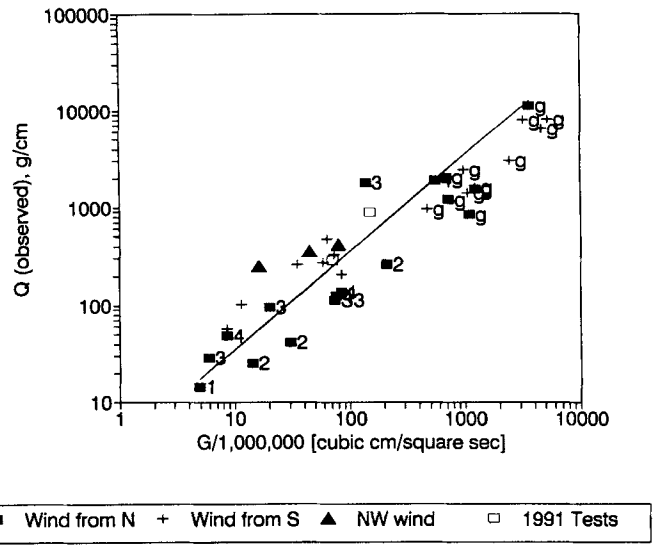

Figure 11. Q versus G for selected data: 1, zero point; 2, 50 m south; 3, 100 m south; 4150 m south; S1 520 m south. G values for which u_* exceeded 60 cm s^{-1} are labelled 'g'. The line is the regression equation $Q = 3{\cdot}5 \times 10^{-6}\, G$

tion obtained in the same way as above. Because this location had no detected crust fragments left, it does not show a progression of a higher to a lower u_{*t} resulting from sandblasting of soil aggregates. The u_{*t} estimate of approximately 16 cm s^{-1} is consistent with fine sand surfaces with no aggregation.

q versus $u_*(u_*^2 - u_{*t}^2)$

Figure 11 shows integrals in time of q versus $u_*(u_*^2 - u_{*t}^2)$ (Q versus G) for the data sets used in the friction velocity section as well as the preliminary data set obtained in 1991 (two points of data), and the data sets obtained on 17 March (wind from the northwest, off axis), 24, 16 and 19 March. The total number of pair values of the time integrals of q versus $u_*(u_*^2 - u_{*t}^2)$ (Q versus G) is 36. For G values in which part of the wind friction velocities were larger than 60 cm s^{-1} the points are labelled g. For the points obtained for north winds and friction velocities less than 60 cm s^{-1}, the linear regression is $Q = 3{\cdot}5 \times 10^{-6}\, G$ with $r^2 = 0.61$ and a standard error of the coefficient of $0{\cdot}67 \times 10^{-6}$.

Referring to Equation 2, this regression constant would correspond to a value for constant A of 2·8 for an assumed $F(x) = 1$. This constant shows reasonable consistency of the data with Equation 2. The greatest source of error for these estimates is the fact that u_{*t} changes continuously but we only measured it once or twice for each G estimate. To identify possible patterns for the residuals, we labelled the locations in Figure 11 as follows: 1 = 0 m; 2 = 50 m; 3 = 100 m; 4 = 150 m; S1 = 520 m; S3 = 1057 m.

The distribution of the residuals to the fit for the north wind cases for friction velocities less than 60 cm s^{-1} shows for the zero point and 50 m locations (1 and 2) that the residual is less than zero for five of five cases. For the 100 m and 150 m locations (3 and 4), the residual is greater than zero for four of five cases. For the null hypothesis that the residuals are random with equal probability of being positive or negative and do not increase with distance to the south, the (binomial distribution) probability of the observed residuals (nine of ten) is 0·0107 (Miller and Freund, 1977). Therefore, the null hypothesis is rejected at the 90 per cent level in favour of residuals that do increase with distance to the south. We interpreted this result as a confirmation of the avalanching effect; that is, $F(x)$ in Equation 2 does increase downwind for threshold velocities decreasing downwind.

For Q-G data points representing winds that exceeded friction velocities of 60 cm s^{-1}, Figure 11 shows that G overpredicts the observed Q for the above regression equation $Q = 3{\cdot}5 \times 10^{-6}\, G$. This is consistent with our 520 m data set for 11 March showing Sensit response versus friction velocity flattening out for

friction velocity greater than 60 cm s^{-1}; it appears that the relationship $q = A'u_*(u_*^2 - u_{*t}^2)$ does not apply for $u_* > 60$ cm s^{-1}.

One final feature of Figure 11 is that all but one of the Q–G pairs collected for south winds with friction velocities less than 60 cm s^{-1} were greater than the regression equation for north winds with friction velocities less than 60 cm s^{-1}. We explain this by noting that airborne sand is transported beyond the location of its origin. Thus, an overshoot would be expected when threshold friction velocities are decreasing with fetch. This behaviour is consistent with the theoretical work of Anderson and Haff (1991) and the wind tunnel experimentation of Shao and Raupach (1992) which showed a lag of the order of metres between changes in wind speed and changes in associated fluxes (due to a hop-length response effect).

DISCUSSION

Evidence of the avalanching effect was seen in the present experiment. However, the following observations led us to favour a model that included (in addition to avalanching) the aerodynamic feedback and soil resistance effects.

(1) The increase of aerodynamic roughness height during 09 : 30–11 : 00 LST on 11 March 1993 along with the increase of u_* with distance downwind. This increase was consistent with Owen's theory, which predicted a gradient of friction velocity and q resulting from the saltation-induced increase of aerodynamic roughness height.
(2) A gradient of threshold friction velocity for all wind erosion episodes. The positive gradient of threshold friction with fetch was probably the dominating cause of the decrease of Q with downwind distance on 23 March 1993. On 18 March 1993 the negative gradient of threshold friction velocity was probably the dominating cause of the increase of Q with downwind distance.
(3) A non-random relationship of deviations from the best-fit line of Q versus G with distance downwind. This is interpreted to mean that the $F(x)$ in Equation 2 is significant and increases with x. With the $F(x)$ set to 1, however, Equation 2 explained 61 per cent of the variance observed.
(4) Failure of the pure avalanching model to explain decrease of Q downwind. The pure avalanching model did not pass either of its two tests for explaining the observed fetch effect in our experiment.

The fetch effect is probably dominated by soil resistance and avalanching for wind speeds near threshold and by the aerodynamic feedback mechanism and avalanching for wind speeds greatly in excess of the threshold. The importance of the pre-existing aerodynamic roughness height for the aerodynamic feedback effect was seen in the 1991 data in which friction velocities reached levels in excess of 60 cm s^{-1} (slightly above threshold for the coarse sandy soil of the North Owens Lake site). Even though these friction velocities were close to those for the 11 March 1993 case, no evidence was seen for the aerodynamic feedback mechanism.

Owen's theory (see below) is based on a feedback mechanism with respect to distance downwind in which saltation of particles entirely determines the aerodynamic roughness height [$z_0 = u_*^2/(\beta g)$, where $\beta = 95$] which then acts to increase friction velocity. Table III shows the increase of the saltation-controlled aerodynamic roughness height. The roughness height of 0·1 for the 1991 Owens Lake test surface was already larger than the roughness heights calculated by Owen's formula for friction velocities lower than 100 cm s^{-1}. The need for the saltation roughness height to exceed pre-existing roughness height of the natural surface was explained by Raupach (1991). The existence of a smooth upstream surface would be required for the aerodynamic feedback model to dominate. Such was not the case in our experiment in 1991, but on 11 March

Table III. Relation between friction velocity u_* and aerodynamic roughness height z_0, according to the theory of P. R. Owen

u_* (cm s^{-1})	20	40	60	80	100	120	120
z_0 (cm)	0·0043	0·0172	0·0387	0·0687	0·1074	0·1547	0·2105

1993 the finer surface material pulverized into a smooth surface where saltation could generate a z_0 larger than that already present. Table I shows the sediment size distribution of mass for particles between 1 and 2 mm to be 23·3 per cent for the 1991 site and less than 3 per cent for the 11 sediments for the 1993 test sites.

An explanation for the sensitivity for friction velocities close to the threshold is given as a variation of Equation 8. The fractional increase of q may be expressed as a function of the fractional change of threshold friction velocity and friction velocity by the expression

$$\Delta q/q = [3y - B^2y + 2Bs]/(1 - B^2)$$

where $B = u_{*t}/u_*$, $y = \Delta u_*/u_*$, and $s = \Delta u_{*t}/u_*$. The sensitivity of the increase of q for a change in u_{*t} and u_* is always greatest for friction velocity near the threshold. For example, for $B = 0{\cdot}95$, the fraction of change of q for a 10 per cent change of threshold friction velocity is 1·95. It is also seen for u_* greater than u_{*t} (small B) that the change of friction velocity dominates.

Except for periods of about 2 h, our data did not show any significant change of aerodynamic roughness height with distance downwind. This observation would imply that the partially destroyed crust provided a relatively homogeneous roughness even though the portion of aggregated material (crustal pieces) to loose sand changed along the fetch. We took this to mean that no internal boundary layers were forming during our experimental time except during 2 h on 11 March 1993. During the 2 h when our data suggest that aerodynamic roughness height as well as friction velocity increases with distance (9 : 30–11 : 30 on 11 March), the goodness of fit of the logarithmic profile would imply that the ratio of separation distance to tower height (50/3) was sufficient and that the increase of z_0 with distance downwind was such as to support our conclusion that the data *suggest* an increase of z_0 with distance downwind and that z_0 is significantly larger during the peak of the windstorm than 2 h previous to or following the peak.

The failure of the constancy of Q/G for large friction velocities has been verified by independent wind tunnel tests of Rasmussen and Iversen (pers. comm., March 1994). The cause of this failure is not fully known at this time.

Our data showed that the threshold friction velocity changes with time as well as distance as saltation successively destroys the aggregate structure of the soil. For a complete description of the fetch effect, it is necessary to know both soil physical state and wind stress and to predict the destruction of soil aggregates by saltation.

CONCLUSION

The data lead us to a conditional acceptance of a model (Equation 2) having three mechanisms that cause the wind erosion fetch effect: avalanching, soil resistance, and aerodynamic feedback. Aerodynamic feedback occurred at one location but not another for similarly strong winds. Differences in pre-existing aerodynamic roughness height reflecting differences in the sediment caused this difference in response. For the conditions present at the Owens Lake test site in March 1993, progressive disintegration of soil crust by sandblasting from north to south caused a decrease of threshold friction velocity with distance south from the unbroken crust. The gradient of threshold friction velocity contributed to an opposite gradient of soil flux. Finally, the avalanching effect is important for small-scale (of the order of a few metres) wind erosion fetch effects. At the leading edge separating non-erodible material from erodible material, it is a dominating effect. For scales of more than 50–100 m, however, it is a residual effect, responsible for a small fraction of the total fetch effect. The dominating large-scale (greater than 100 m) fetch effect mechanism for all but about 2 h during the March 1993 study was the variation of threshold velocity on the surface of the lake.

Although the conditions of Owens Lake are unusual in some respects, the experiment was undertaken in terms of general physical properties: wind stress and soil resistance to erosion measured in terms of friction velocity and threshold friction velocity, respectively. Since threshold friction velocity is a function of soil composition and size distribution, and friction velocity is a function of pressure gradients, topography and roughness, the experimental results may be applied to a wide variety of environments. For example, for a non-aggregated, monodisperse sand (leading to homogeneous threshold velocity), the fetch effect

would be primarily controlled by the Owen's effect and secondarily by avalanching. For fields where non-homogeneities in size distribution of particles lead to inhomogeneous threshold velocity (by aggregation differences or non-aggregated size distributions) the threshold effect could be the primary control of the fetch effect, with Owen's effect and avalanching as secondary controls.

Field observations of friction velocity and soil flux led us to confirm Owen's formula $q = A'(u_*(u_*^2 - u_{*t}^2)$ for friction velocities smaller than 60 cm s^{-1}. Our field observations agreed with measurements made in wind tunnels for friction velocities greater than 60 cm s^{-1}, which showed that q increases with u_* at a rate less than the Owen's formula.

ACKNOWLEDGEMENTS

The authors are pleased to acknowledge Trevor Ley, whose tireless work made the Lake Owens Dust Experiment (LODE) possible. Rolf Kihl of the Institute of Arctic and Alpine Research of the University of Colorado described soil properties. Bill Cox, Duane Ono, and Grace Holder of the Unified Great Basin Air Pollution Control District were very helpful in finding the experimental site. Estimation of percentage of surface as crust was done by Millinda Vialpondo. Mr Michael Patterson of Swansea, California, was a consultant and invaluable asset to the LODE. This work was funded in part by California Air Resources Board Contract No. A132105. The statements and conclusion are not necessarily those of the California Air Resources Board. The mention of commercial products does not constitute an endorsement by NOAA or the CARB.

P. R. Owen finished a short manuscript before his death in which he modelled a fetch effect caused by adjustment of an internal boundary layer to erodible material having u_* for an aerodynamically smooth upwind surface and a rough upwind surface. This note follows. Unfortunately, no other supporting material for the aerodynamically caused fetch effect was left to us by Prof. Owen.

A THEORY FOR THE 'FIELD LENGTH' EFFECT

P. R. Owen (deceased)

When wind, blowing steadily over a passive surface that is either aerodynamically smooth, such as solid rock, or rough, such as vegetated field or a field covered by stubble, encounters an expanse of erodible soil, it sets that soil into a saltating motion. When saltation occurs, it acts on the wind outside the region of particle motion in a way similar to that of solid roughness (Owen, 1964). In general, the magnitude of that roughness differs from the magnitude of an existing roughness on the upstream passive surface, with the consequence that the wind is sensible of an abrupt change in boundary condition. Its friction velocity near the mobile surface is altered, thus modifying the velocity profile in the airstream.

Such alterations to the flow are not communicated immediately to the whole of the planetary boundary layer, but are confined to an internal boundary layer that grows with increasing distance downstream from the leading edge of the mobile deposit. The object of the theory is to calculate the development of the friction velocity in the direction of the flow. Accordingly, the problem exhibits a similarity to that encountered in meteorology when wind blows over terrain whose roughness changes. The present calculation, however, contains an essential complication arising from the fact that, whilst the saltation-induced roughness of the ground is dependent on the friction velocity in the wind, the development of that friction velocity, indeed of the entire flow within the internal boundary layer, is controlled by the same saltation-induced roughness, hence coupling the equations governing the airflow with those for the saltation.

It is supposed that the roughness height z_0 on the passive surface is known, as is u_{*t}, the friction velocity in the undisturbed wind, whose velocity profile is taken to be logarithmic. A value of z_0 may also be ascribed to a smooth surface, and is proportional to ν/u_{*1} where ν is kinematic viscosity. Downstream from the roughness discontinuity, the conservation conditions on the mass flux of air and its momentum enable the flow to be determined.

A restriction on the results arises from the implicit condition that, when the upstream surface is rough, z_0

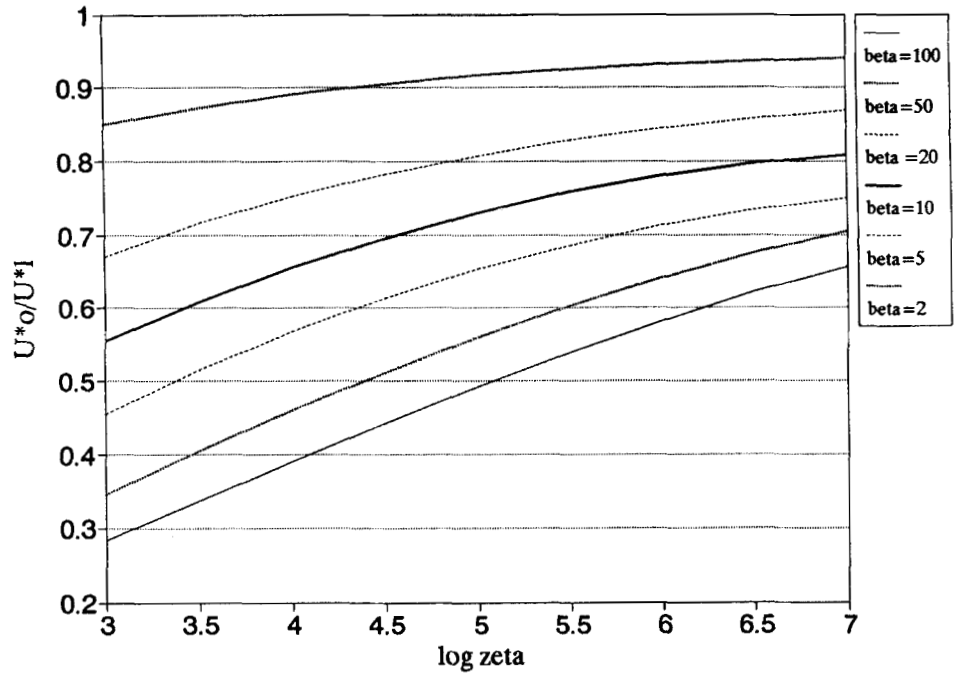

Figure A. Development of the friction velocity over a mobile surface preceded by a rough passive surface. Zeta = $15{\cdot}5\,gx/u_{*1}^2$, where g is gravitational acceleration, x is horizontal distance downwind of the leading edge, and u_{*1} is friction velocity just upwind of the leading edge. Beta = $97\,gz_0/u_{*1}^2$, where z_0 is the aerodynamic roughness height just upwind of the leading edge

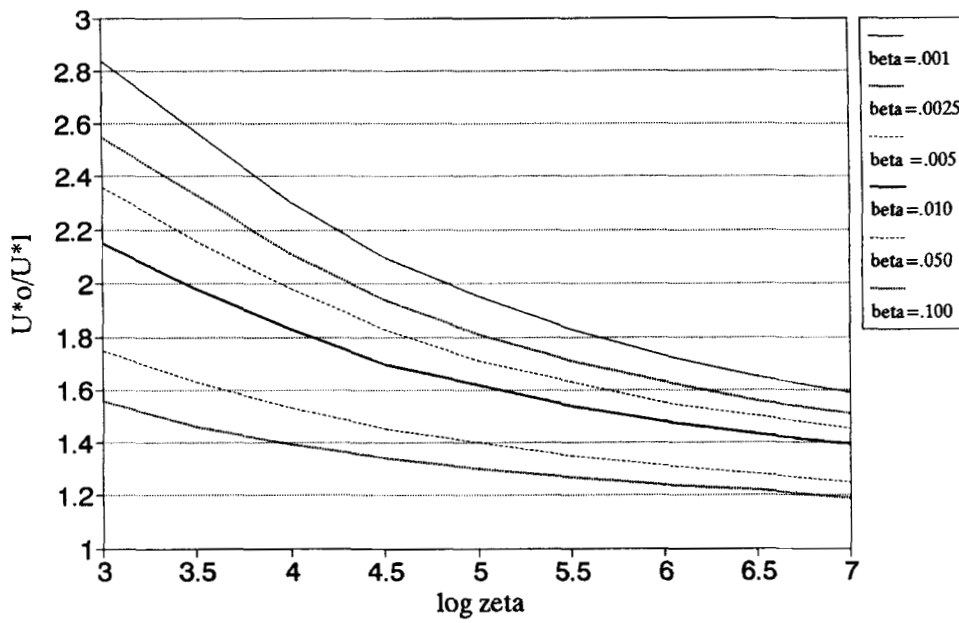

Figure B. Development of the friction velocity over a mobile surface preceded by a smooth passive surface. Zeta = $15{\cdot}5\,gx/u_{*1}^2$, where g is gravitational acceleration, x is horizontal distance downwind of the leading edge, and u_{*1} is friction velocity just upwind of the leading edge. Beta = $13{\cdot}1g\nu/u_{*1}^3$, where z_0 is the aerodynamic roughness height just upwind of the leading edge and ν is kinematic viscosity

must exceed a certain minimum in u_{*1}, or in β ($= 97gz_0/u_{*1}^2$), so as to ensure that saltation can occur at the leading edge of the mobile deposit. The corresponding values of $z_{0\min}$ are as follows:

β	2	3	10	20	40	50	100
$z_{0\min}$ (cm)	0·009	0·019	0·116	0·302	0·754	1·006	2·425

The development of u_*/u_{*1}, where $u_*(x)$ is the friction velocity over the saltation, ceases when the internal boundary layer reaches the top of the planetary boundary layer, taken to be approximately $0{\cdot}2\,u_*/f$, where f is the Coriolis parameter in the atmosphere.

Numerical results are presented in Figure A for a rough surface. In conjunction with the flux equation above, it evidently reproduces the effect described by Chepil (1946) as 'avalanching', wherein the particulate flux increases with distance downstream from the leading edge of the eroding surface. Were the passive surface smooth, Figure B indicates an opposite behaviour, the flux decreasing in the downstream direction.

REFERENCES

Anderson, R. and Haff, P. 1991. 'Wind modification and bed response during saltation of sand in air', *Acta Mech.*, suppl. 1, 21–51.

Bradley, E. F. 1968. 'A micrometeorological study of velocity profiles and surface drag in the region modified by a change in surface roughness'. *Quart. J. Roy. Meteorol. Soc.*, **94**, 361–379.

Cahill, T. A., Gill, T. E., Reid, J. S., Gearhart, E. A. and Gillette, D. A. 1996. 'Saltating particles, playa crusts and dust aerosols from Owens (dry) Lake, California, *Earth Surface Processes and Landforms.*

Chepil, W. S. 1946. 'Dynamics of wind erosion, V. Cumulative intensity of soil drifting across eroding fields', *Soil Sci.*, **61**, 257–263.

Chepil, W. S. 1957. *Width of field strips to control wind erosion*, Kansas State Agricultural Experiment Station Tech. Bull., **92**.

Chepil, W. S. and Milne, R. A. 1939, 'Comparative study of soil drifting in the field and in a wind tunnel', *Sci. Agric.*, **249**.

Fryrear, D. W. 1986. 'A field dust sampler', *J. Soil Water Conserv.*, **41**, 117–120.

Gillette, D. A. and Stockton, P. H. 1989. 'The effect of nonerodible particles on wind erosion of erodible surfaces', *J. Geophys. Res.*, **94**, 12, 885–12, 893.

Gillette, D. A., Adams, J., Muhs, D. and Kihl, R. 1982. 'Threshold friction velocities and rupture moduli for crusted desert soils for the input of soil particles into the air', *J. Geophys. Res.*, **87**, 9003–9015.

Gregory, J. M. and Borrelli, J. 1986. *The Texas Tech wind erosion equation*, American Society of Agricultural Engineers, Paper No. **86-2528**.

Miller, I. and Freund, J. 1977. *Probability and Statistics for Engineers, 2nd edn*, Prentice-Hall, Englewood Cliffs, New Jersey.

Owen, P. R. 1964. 'Saltation of uniform sand grains in air', *J. Fluid Mech.*, **20**, 225–242.

Panofsky, H. and Dutton, J. 1984. *Atmospheric Turbulence Models and Methods for Engineering Applications*, Wiley Interscience, New York, p. 129.

Pomeroy, J. W., Gray, D. M. and Landine, P. G. 1993. 'The prairie blowing snow model: characteristics, validation, operation'. *J. Hydrology*, **144**, 165–192.

Raupach, M. 1991. 'Saltation layers, vegetation canopies and roughness lengths', *Acta Mechanica* (Suppl) **1**, 83–96.

Shao, Y. and Raupach, M. R. 1992. 'The overshoot and equilibrium of saltation', *J. Geophys. Res.* **97**, 20, 559–564.

Shao, Y., McTainsh, G., Leys, J. and Raupach, M. 1993. 'Efficiencies of sediment samplers for wind erosion measurements'. *Aust. J. Soil Res.*, **31**, 519–32.

Stockton, P. H. and Gillette, D. A. 1990. 'Field measurement of the sheltering effect of vegetation on erodible land surfaces', *Land Degrad. Rehabil.*, **2**, 77–85.

Stout, J. E., 1990. 'Wind erosion within a simple field', *Trans. Am. Soc. Agric. Eng.*, **33**, 1597–1600.